

¹ Fractional advection-dispersion equations for ² modeling transport at the Earth surface

Rina Schumer

³ Desert Research Institute, Reno, NV, USA

Mark M. Meerschaert

⁴ Michigan State University, East Lansing, MI, USA

Boris Baeumer

⁵ University of Otago, Dunedin, NZ

Rina Schumer, Division of Hydrologic Sciences, Desert Research Institute, Reno, NV, 89512, USA.(rina@dri.edu)

Mark M. Meerschaert, Department of Statistics and Probability, Michigan State University, East Lansing, MI, 48824, USA. (mcubed@stt.msu.edu)

Boris Baeumer, Department of Mathematics and Statistics, University of Otago, Dunedin, NZ(bbaeumer@maths.otago.ac.nz)

6 **Abstract.** Characterizing the collective behavior of particle transport on
7 the Earth surface is a key ingredient in describing landscape evolution. We
8 seek equations that capture essential features of transport of an ensemble
9 of particles on hillslopes, valleys, river channels, or river networks, such as
10 mass conservation, super-diffusive spreading in flow fields with large veloc-
11 ity variation, or retardation due to particle trapping. Development of stochas-
12 tic partial differential equations such as the advection-dispersion equation
13 (ADE) begin with assumptions about the random behavior of a single par-
14 ticle: possible velocities it may experience in a flow field and the length of
15 time it may be immobilized. When assumptions underlying the ADE are re-
16 laxed, a fractional ADE can arise, with a non-integer order derivative on time
17 or space terms. Fractional ADEs are non-local; they describe transport af-
18 fected by hydraulic conditions at a distance. Space fractional ADEs arise when
19 velocity variations are heavy-tailed and describe particle motion that accounts
20 for variation in the flow field over the entire system. Time fractional ADEs
21 arise as a result of power law particle residence time distributions and de-
22 scribe particle motion with memory in time. Here we present a phenomeno-
23 logical discussion of how particle transport behavior may be parsimoniously
24 described by a fADE, consistent with evidence of super-diffusive and sub-
25 diffusive behavior in natural and experimental systems.

1. Introduction

26 An important class of problems in the Earth-surface sciences involves describing the
27 collective behavior of particles in transport. Familiar examples include transport of solute
28 and contaminant particles in surface and subsurface water flows, the behavior of soil
29 particles and associated soil constituents undergoing biomechanical transport and mixing
30 by bioturbation, and the transport of sediment particles and sediment-borne substances
31 in turbulent shear flows, whether involving shallow flows over soils, deeper river flows, or
32 ocean currents. These and many other examples share three essential features. First, is
33 the behavior of a well defined ensemble of particles. These particles may be considered
34 tracers whose total mass is conserved or otherwise accounted for if radioactive decay,
35 physical transformations or chemical reactions are involved. Second, these tracers typically
36 alternate between states of motion and rest over many time scales, and indeed, most
37 tracers of interest in Earth-surface systems are at rest much of the time. Third, when in
38 transport, some tracers move faster, and some move slower, than the average motion due
39 to spatiotemporal variations in the mechanisms inducing their motion. Tracer motions
40 thus may be considered as consisting of quasi-random walks with rest periods.

41 During motion, tracers may experience characteristically different ‘hop’ or ‘jump’ be-
42 haviors. Consider releasing at some instant an ensemble of tracers within a system, say,
43 marked particles within a river. Assuming all tracers undergo and remain in motion, then
44 due to turbulence fluctuations in the case of suspended particles, or to effects of near-
45 bed turbulence excursions together with tracer-bed interactions in the case of bedload
46 particles, during a small interval of time Δt , most of the tracers move short distances

47 downstream whereas a few move longer distances. The displacement (or hop) distance
48 Δx generally may be considered a random variable. If the probability density function
49 (pdf) describing hop length has a form that declines at least as fast as an exponential
50 distribution, then it possesses finite mean and variance. Moreover, after finite time t ,
51 the center of mass of the tracers is centered at the position $x = x_0 + vt$, where x_0 is
52 the starting position and v is the mean tracer speed. The spread or ‘dispersion’ around
53 average tracer position, described by standard deviation, grows at a constant rate with
54 time $\sigma = (Dt)^{1/2}$ where D is the dispersion coefficient. As described below, this behavior
55 known as Fickian or Boltzmann scaling may be characterized as being ‘local’, in that dur-
56 ing a small interval, tracers in motion mostly move from location x to nearby positions.
57 Conversely, during the same interval, tracers arriving at position x mostly originate from
58 nearby positions. Letting $C(x, t)$ denote the local tracer concentration, then in this local
59 case the behavior of C may be adequately described by the classic advection-dispersion
60 equation (ADE).

61 Consider, in contrast, the possibility that the hop length pdf declines with distance in
62 such a way that the variance is undefined, for example, a power-law distribution. In this
63 case, long displacement distances, albeit relatively rare, are nonetheless more numerous
64 than with, say, an exponential distribution - so that hop length density possesses a so-
65 called ‘heavy tail’. For example, during downstream transport, sediment tracers dispersed
66 by turbulent eddies and by momentary excursions into parts of the mean flow that are
67 either faster or slower than the average may occasionally experience super dispersive events
68 during excursions into sites with unusually high flow velocities [Bradley *et al.*, 2009]. In
69 these situations where the hop length density is heavy-tailed, the scaling of dispersion

70 is non-Fickian, that is, $\sigma = (Dt)^{1/\alpha}$, where $1 < \alpha < 2$. Because σ therefore grows
71 at a rate faster than ‘normal’ Fickian dispersion, this behavior is referred to as ‘super-
72 diffusive’. Moreover, this behavior may be characterized as being ‘nonlocal’ in that during
73 a small interval, tracers released from position x mostly move to nearby positions, but
74 also involve an ‘unusually large’ number of motions to positions far from x . Conversely,
75 during the same interval, tracers arriving at position x mostly originate from nearby
76 positions, but also involve a significant number of motions originating far from x . This
77 means that the behavior at a particular position does not necessarily depend only on local
78 (nearby) conditions, but rather may also depend on conditions upstream or downstream.
79 For example, because the local rate of change in tracer concentration consists of the
80 divergence of the flux of tracers, then if the flux is related to the bed stress, say, in the
81 case of sediment transport, the possibility exists that changes in the local concentration
82 depend on stress conditions and therefore on system configuration ‘far’ upstream. As
83 described below, the behavior of the tracer concentration $C(x, t)$ in this ‘nonlocal’ case
84 may be described by a fractional derivative version of the advection-dispersion equation.

85 Consider now an ensemble of tracers whose motions, after release, involve states of
86 motion and rest. In the case of tracer particles moving as bedload, rest states might involve
87 momentary disentrainment on the bed surface associated with turbulence fluctuations, or
88 burial beneath the surface for longer periods followed by reentrainment with scour [*Nikora*
89 *et al.*, 2002; *Parker et al.*, 2000]. Even longer rest periods might consist of storage of
90 tracers within the bars and floodplain of a river [*Malmon et al.*, 2002, 2003]. Similarly,
91 rest times of nutrients in open-channel flow might consist of temporary excursions into
92 so-called dead zones, or into hyporheic zone storage, with eventual release back into the

93 main fluid column [*Haggerty et al.*, 2002; *Gooseff et al.*, 2003]. With bioturbation of
94 soil particles, rest times consist of the intervals between displacement by biotic activity.
95 The rest time (or waiting time, or residence time) may be considered a random variable.
96 If random waiting times are, in general, small, then the speed V may be considered an
97 average virtual speed that includes periods of motion and rest, and the local rate of change
98 in tracer concentration, $\frac{\partial C}{\partial t}$, in the ADE accommodates this. If, in contrast the waiting
99 time density is a heavy-tailed distribution that reflects the presence of unusually long
100 rest periods for tracers in storage, then as described below a suitable phenomenological
101 description of the behavior of the tracer concentration $C(x, t)$ may be obtained from a
102 fractional ADE (fADE) with a fractional time term $\frac{\partial^\gamma C}{\partial t^\gamma}$, where $0 < \gamma < 1$. Dispersion
103 now scales at a rate proportional to $t^{\gamma/2}$. Because σ grows at a rate slower than normal
104 Fickian dispersion, this behavior is referred to as sub-diffusion. This characterizes a long
105 memory effect, analogous to an influence from ‘far’ upstream as described above with
106 reference to the fractional space derivative; the fractional time derivative characterizes an
107 influence from far back in time. Like variations in tracer speed, rest times contribute to
108 dispersion. As such, these effects may not be separable without ancillary information.

109 As elaborated below, if both the hop length density and the waiting time density are
110 heavy-tailed, then the fADE can include both a time and a space fractional derivative.
111 Dispersion now scales at a rate proportional to $t^{\gamma/\alpha}$. Note that a particular value of the
112 ratio $\frac{\gamma}{\alpha}$ is a non-unique combination of values of α and γ . This means that if the ratio
113 is obtained empirically from measurements of tracer dispersion, say, in a flume or river,
114 additional information empirical and/or theoretical is needed to distinguish whether the
115 source of the anomalous dispersion resides with the hop lengths, waiting times, or both.

116 On this note we point out that the development below provides a mostly phenomenological
117 viewpoint of how tracer behavior may be parsimoniously described by a fADE, consistent
118 with evidence of super-diffusive and sub-diffusive behavior in natural and experimental
119 systems (e.g. *Benson et al.* [2001, 2000]; *Haggerty et al.* [2002]; *Schumer et al.* [2003]). A
120 particularly exciting opportunity resides in clarifying the underlying physics that lead to
121 these behaviors, including the mechanisms that give rise to heavy-tail distributions of hop
122 distances and waiting times, perhaps building on recent insights from the hydrologic liter-
123 ature. In the following sections, we look at details underlying the application of fractional
124 advection-dispersion equations for describing collective behavior of particle transport at
125 the Earth surface. Much of this manuscript is a review of basic information about fADE
126 for non-specialists that is not available in a single reference. New material fills in theoret-
127 ical gaps, compares solution characteristics and application of various fADEs, and links
128 landscape evolution processes to the conceptual models underlying fADEs.

2. Fractional Derivatives

129 Before presenting fractional ADEs, we provide some useful introductory material about
130 fractional derivatives. Three characteristics of fractional derivatives will be used to in-
131 terpret and solve fractional ADEs: (1) the Grunwald fractional difference quotient that
132 approximates a fractional derivative; (2) the fractional derivative as the convolution of
133 an integer-order derivative with a memory function; and (3) the Fourier and Laplace
134 transforms of fractional derivatives.

2.1. Grunwald finite difference

135 How can we generalize our understanding of derivatives to include non-integer order
136 cases? The first derivative of a function $y = f(x)$ is approximated by the difference
137 quotient $\Delta y/\Delta x$ where $\Delta x = h$ and $\Delta y = f(x) - f(x - h)$ (Fig. 1(a)). The second
138 derivative $f''(x)$ is approximated by $\Delta^2 y/\Delta x^2$ where

$$\begin{aligned} \Delta^2 y &= \Delta[f(x) - f(x - h)] \\ &= [f(x) - f(x - h)] - [f(x - h) - f(x - 2h)] \\ &= f(x) - 2f(x - h) + f(x - 2h) \end{aligned} \tag{1}$$

140 the second difference. Continuing in this manner shows that the n th order derivative is
141 approximated by the n th finite difference quotient

$$\frac{d^n}{dx^n} f(x) \approx \frac{1}{h^n} \sum_{j=0}^n \binom{n}{j} (-1)^j f(x - jh) \tag{2}$$

143 where the binomial coefficients (from Pascal's triangle)

$$\binom{n}{j} = \frac{n!}{j!(n-j)!} = \frac{\Gamma(n+1)}{\Gamma(j+1)\Gamma(n-j)}.$$

145 The Grunwald definition of the fractional derivative is the non-integer variant of (2)

$$\frac{d^\alpha}{dx^\alpha} f(x) \approx \frac{1}{h^\alpha} \sum_{j=0}^{\infty} \binom{\alpha}{j} (-1)^j f(x - jh) \tag{3}$$

147 where the fractional binomial coefficients are

$$\binom{\alpha}{j} = \frac{\Gamma(\alpha+1)}{\Gamma(j+1)\Gamma(\alpha-j)}$$

149 and the approximation becomes exact as $h = \Delta x \rightarrow 0$. To see that the integer order
150 formula (2) is really a special case of the fractional formula (3), note that the binomial
151 coefficients are $0 = 1/\infty$ for $j > n$, so that we could have written the sum in (2) with the
152 upper limit of infinity.

153 Several interesting properties of the fractional derivative follow from the Grunwald
154 definition (3). Most important is that a fractional derivative is a non-local oper-
155 ator that depends on function values far away from x (Fig. 1(b)). The impor-
156 tance given to a far away point $x - jh$ is measured by the Grunwald weight $w_j =$
157 $(-1)^j \Gamma(\alpha + 1) / (\Gamma(j + 1) \cdot \Gamma(\alpha - j))$ so that $w_0 = 1$, $w_1 = -\alpha$, $w_2 = \alpha(\alpha - 1)/2$ and
158 $w_{j+1} = w_j \cdot (j - \alpha) / (j + 1)$. An appeal to Stirling's approximation [Meerschaert and
159 Scheffler, 2002a] shows that $w_j \approx j^{-(1+\alpha)} / \Gamma(-\alpha)$ (Figure 1). Hence the Grunwald defini-
160 tion is essentially a discrete convolution with a power law. The finite difference formula
161 (3) is also the basis for numerical codes to solve the fractional ADE [Tadjeran et al., 2006].

2.2. Convolution of the derivative with a power-law memory function

162 The continuum limit of the Grunwald finite difference formula is a convolution integral
163 (see for example Meerschaert and Tadjeran [2004]). Writing (3) in terms of the Grunwald
164 weights and using $w_j \approx j^{-(1+\alpha)} / \Gamma(-\alpha)$ shows that

$$\begin{aligned}
 \frac{d^\alpha}{dx^\alpha} f(x) &\approx \frac{1}{\Gamma(-\alpha)} \sum_{j=0}^{\infty} f(x - jh) (jh)^{-\alpha-1} h \\
 &\approx \frac{1}{\Gamma(-\alpha)} \int_0^{\infty} f(x - y) y^{-\alpha-1} dy
 \end{aligned}
 \tag{4}$$

166 which can be written in various equivalent forms [Samko et al., 1993; Mainardi, 1997]. If
167 $f(t)$ is defined on $t \geq 0$ then integration by parts yields the Caputo form

$$\frac{d^\alpha}{dt^\alpha} f(t) = \frac{1}{\Gamma(1 - \alpha)} \int_0^t f'(t - y) y^{-\alpha} dy
 \tag{5}$$

169 which is very useful for fractional time derivatives. Noting that the integral (5) is a
170 convolution we can write

$$\frac{d^\alpha f(t)}{dt^\alpha} = \frac{df(t)}{dt} \star \frac{t^{-\alpha}}{\Gamma(1 - \alpha)}
 \tag{6}$$

172 which relates the fractional derivative to a power-law memory function.

2.3. Transforms of fractional derivatives

173 For partial differential equations, it is useful to use Fourier transforms in space and
174 Laplace transforms in time. Since the transform of a power law is another power law, it
175 is easy to check using (4) and (6) the Fourier and Laplace transforms pairs:

$$\begin{aligned} \frac{d^\alpha f(x)}{dx^\alpha} &\leftrightarrow (ik)^\alpha \hat{f}(k) \\ \frac{d^\gamma f(t)}{dt^\gamma} &\leftrightarrow s^\gamma \tilde{f}(s) - s^{\gamma-1} f(0) \end{aligned} \tag{7}$$

176
177 using $t^{-\gamma}/\Gamma(1-\gamma) \leftrightarrow s^{\gamma-1}$.

2.4. Examples of fractional derivatives

178 Use the Laplace transform pair $t^{-\gamma}/\Gamma(1-\gamma) \leftrightarrow s^{\gamma-1}$ along with the Laplace transform
179 (7) to check that the α -order fractional derivative of t^p is $t^{p-\alpha}\Gamma(p+1)/\Gamma(p+1-\alpha)$ which
180 reduces to the usual form when α is an integer. The Fourier transform (7) can be used
181 to show that the α order fractional derivative of $\sin x$ is $\sin(x + \pi\alpha/2)$, which reduces
182 to the usual formula for integer α using standard trigonometric identities. The α order
183 fractional derivative of e^{bx} is $b^\alpha e^{bx}$ and so forth. The point is that fractional derivatives
184 are natural analogues of their integer order cousins.

3. The classical random walk, central limit theorem, and the ADE

185 Sediment transport has long been modeled as a stochastic sequence of hops and rest
186 periods [*Einstein*, 1937; *Sayre and Hubbell*, 1965] leading to emergent properties after
187 long time. It is also common to represent Earth surface transport process using diffusion-
188 type models arising from the combination of a continuity equation with transport (flux)
189 laws (since *Culling* [1960]). Random walk and diffusion models are related. Specifically,
190 diffusion equations govern the stochastic processes that arise when the scaling limit of

191 random walk is taken. Here we describe the type of particle motion that may be well-
192 modeled by a classical ADE so that the exact nature of our fractional generalizations will
193 be clear. We can approach the advection-dispersion equation from either a Lagrangian
194 or Eulerian point of view. By using a Lagrangian (following the progress of an individual
195 particle with time) approach, the exact nature of the transport process is clarified.

3.1. Lagrangian approach to the ADE

196 Our goal is to describe the motion of an ensemble of particles as measured by its
197 concentration (or mass) in space and time $C(x, t)$. The distribution of particles within the
198 plume will be represented by the pdf governing the location of a single particle in space.
199 The discrete stochastic model we choose to develop this distribution is the random walk.
200 We write the random particle location $X(t)$ as sum of stationary random jump lengths Y_i
201 separated by time steps of length Δt :

$$202 \quad X(t) = \sum_{n=1}^{t/\Delta t} Y_n.$$

203 Then we can use the Central Limit Theorem (CLT) to estimate the distribution of $X(t)$
204 at long time. The law of large numbers (LLN) says that the average of independent and
205 identically distributed (iid) random variables with mean μ converges to the theoretical
206 average:

$$207 \quad \frac{Y_1 + \dots + Y_n}{n} - \mu \rightarrow 0 \quad (8)$$

208 as n becomes large. The CLT refines this statement by approximating the deviation
209 between these two terms. It says that when appropriately rescaled, the sum of iid ran-
210 dom variables with mean μ and standard deviation σ converges to a standard normal

211 distribution:

$$212 \quad \frac{Y_1 + \cdots + Y_n - n\mu}{\sigma n^{1/2}} \rightarrow N(0, 1)$$

213 We use this theorem to approximate the sum of iid particle jumps

$$214 \quad Y_1 + \cdots + Y_n \approx n\mu + \sigma n^{1/2} N(0, 1). \quad (9)$$

215 Let the number of jumps be the total time divided by time per jump $n = \frac{t}{\Delta t}$ and recast
216 the CLT to suit the random sum

$$217 \quad Y_1 + \cdots + Y_n \approx t \frac{\mu}{\Delta t} + \frac{\sigma}{\sqrt{\Delta t}} t^{1/2} N(0, 1). \quad (10)$$

218 Let $v = \frac{\mu}{\Delta t}$ and $D = \frac{\sigma^2}{2\Delta t}$ and we find a Gaussian density

$$219 \quad C(x, t) = \frac{1}{\sqrt{2\pi \cdot 2Dt}} e^{-\frac{(x-vt)^2}{2 \cdot 2Dt}} \quad (11)$$

220 that governs particle location after a number of jumps. The right-hand side of (10) is
221 called Brownian motion with drift. It combines a deterministic advective drift with a
222 stochastic diffusion term $Z(t) = (2Dt)^{1/2} N(0, 1)$ that spreads like $t^{1/2}$ (Fickian scaling).
223 The ADE solution $C(x, t)$ given by (11) is the probability density of the process $vt + Z(t)$
224 that represents the location of a randomly selected particle at time $t > 0$, assuming
225 that particle location $x = 0$ at the initial time $t = 0$. Figure 2(a) illustrates the simple
226 random walk. Figure 2(b) shows the same random walk at a longer time scale. Figure
227 2(c) shows the Brownian motion that emerges as the long-time scaling limit of this simple
228 random walk. The continuous graph of the particle path is a random (not generated from
229 a deterministic pattern) fractal with Hausdorff dimension $3/2$ [*Mandelbrot*, 1982]. The
230 abrupt jumps seen in the random walk disappear in the scaling limit. Figure 3 illustrates
231 the probability density $C(x, t)$ of particle locations for the Brownian motion limit process.

3.2. Eulerian approach to the ADE

232 Using an Eulerian approach, we choose a specific location in space and describe particle
233 motion through that location with time. From this perspective, we begin with a conser-
234 vation of particle mass equation that equates the rate of mass change at a location with
235 the difference between the mass of particles entering and leaving:

$$236 \quad n \frac{\partial C(x, t)}{\partial t} = - \frac{\partial F(x, t)}{\partial x}, \quad (12)$$

237 where effective porosity $n = 1$ for transport at the surface, particle concentration C is in
238 mass per volume, and flux F in mass per area per time. If particle flux is assumed to be
239 by advection and Fickian dispersion:

$$240 \quad F = vnC - n\mathcal{D} \frac{\partial C}{\partial x}, \quad (13)$$

241 where v is average particle velocity and \mathcal{D} is a dispersion coefficient, then we obtain the
242 advection-dispersion equation (also known as the Fokker Planck equation [*Feller*, 1971]):

$$243 \quad \frac{\partial C(x, t)}{\partial t} = -v \frac{\partial C}{\partial x} + \mathcal{D} \frac{\partial^2 C(x, t)}{\partial x^2}. \quad (14)$$

244 The solution to the ADE can be obtained using Fourier transforms:

$$245 \quad \frac{\partial \hat{C}(k, t)}{\partial t} = -v(ik)\hat{C}(k, t) + \mathcal{D}(ik)^2\hat{C}(k, t). \quad (15)$$

246 Solve for C and use initial conditions $C(x, 0) = \delta(0)$ to find

$$247 \quad \hat{C}(k, t) = e^{(-vt(ik) + Dt(ik)^2)} \quad (16)$$

248 the Fourier transform of a Gaussian density (11) with mean $\mu = vt$ and variance $\sigma^2 = 2Dt$.

249 It is interesting that the deterministic solution to a partial differential equation should
250 be a pdf. This important observation means that random behavior exhibits a deterministic
251 regularity at long time. The location $vt + Z(t)$ of a randomly selected particle is unknown,

252 but even so, the relative concentration of particles is predictable. We obtain the same
253 solution using the Eulerian perspective of Fickian particle jumps and conservation of
254 solute mass, or the Lagrangian random walk formulation taken to its scaling limit by
255 applying the CLT. The assumptions underlying the CLT must hold for a Gaussian limit
256 to emerge. This means that there are assumptions buried in Fickian/mass conserving
257 ADE that must hold for it to be applicable. Our focus here is that, in order for the ADE
258 to emerge, there can be only moderate deviation from the average jump size. Since it
259 is well known that the ADE and its solutions do not always reproduce essential features
260 of sediment or solute transport (e.g. *Benson* [1998]; *Ganti et al.* [2009]; *Gooseff et al.*
261 [2003]; *Worman et al.* [2007]; *Neuman and Tartakovsky* [2009], as well as references in
262 this special issue on stochastic transport and emergent scaling at the Earth surface), we
263 will now consider models that allow less stringent assumptions. We will also explore the
264 long memory case where a time component is introduced by allowing random waiting times
265 between jumps. In the following sections, we introduce fractional-in-space ADEs caused
266 by heavy-tailed velocity distributions, and fractional-in-time ADEs caused by heavy-tailed
267 residence times.

3.3. Characteristics of ADE solutions

268 If tracer transport is well modeled by a classical ADE, then long-term transport charac-
269 teristics (of a pulse of tracer) will resemble the Green's function (point source) solutions
270 [*Arfken and Weber*, 1995] to traditional integer-order advection-dispersion equations (Fig.
271 4). These characteristics include:

272 1. Spatial snapshots

273 (i) Gaussian (symmetric bell-shaped) concentration profiles

- 274 (ii) Plume edges decay rapidly
- 275 (iii) Snapshot width spreads like $t^{1/2}$
- 276 (iv) Total mass remains constant over time

277 2. Flux at position x

- 278 (i) Bell-shaped breakthrough curves
- 279 (ii) Leading and trailing edges decay rapidly
- 280 (iii) Breakthrough curve width grows like $x^{1/2}$
- 281 (iv) Area under breakthrough curve remains constant

4. Fractional-in-space ADEs

282 A variety of field and theoretical studies suggest super-diffusive non-locality in transport
283 of tracers at the Earth surface. For example, re-analysis of tracer studies in sand and
284 gravel-bed streams revealed hop length distributions with heavy tails [*Bradley et al.*,
285 2009]. *Foufoula-Georgiou et al.* [2009] argue that transport on hillslopes is non-local
286 and that sediment flux must be calculated using not just the local gradient, but also
287 that of upslope topography. *Stark et al.* [2009] use a fractionally integrated flux term to
288 capture non-local effects in a model of bedrock channel evolution that includes the effect
289 of hillslope sediment production on channel bed sediment buffering and bedrock erosion.
290 These studies all suggest fractional flux terms to represent non-locality in transport.

291 *Hill et al.* [2009] suggest the source of power law hop lengths in bedload transport. They
292 present and review experimental data to justify an exponential step length for particles
293 of a given size. Since mean step length varies with particle size, the overall step length
294 for all particles is a mixture of those exponential distributions. Using standard models

295 [e.g., Gamma distribution] for the pdf of grain size leads to an overall step length pdf
 296 with a heavy power law tail. Even though neither the grain size distribution nor the step
 297 length pdf for grains of a given diameter are heavy tailed, the mixture distribution turns
 298 out to have a heavy tail. This result shows that a fractional Exner equation [*Ganti et*
 299 *al.*, 2009] is applicable to bedload transport. It also highlights the need for additional
 300 experiments and analysis to improve estimates of grain size distribution, step length for
 301 moving particles, as well as entrainment rate for particles of varying size. Here we develop
 302 space-fractional ADEs used to model super-diffusive transport using both the Lagrangian
 303 (particle tracking) and Eulerian (conservation of mass) approach.

4.1. Lagrangian approach to fractional-in-space ADEs

304 If the density of jump lengths Y_i is the heavy-tailed density $p(x)$, then the integral
 305 $\sigma^2 = \int_{-\infty}^{\infty} (Y_i - \mu)^2 p(x) dx$ diverges. Then the classical CLT we use to determine the
 306 density of the sum of jump lengths $X(t)$ does not hold. A more general form of the CLT
 307 exists, however, and says that the properly rescaled sum of stationary iid random variables
 308 with even infinite variance converges in distribution to an α -stable density, denoted S_α ,
 309 with mean μ , spread σ , tail parameter α , and skewness β [*Feller*, 1971; *Gnedenko and*
 310 *Kolmogorov*, 1968]. Here we assume that particle jumps are heavy-tailed in the direction
 311 of flow only.

$$312 \quad \frac{X_1 + \cdots + X_n - n\mu}{\sigma n^{1/\alpha}} \rightarrow S_\alpha(\mu = 0, \sigma = 1, \alpha, \beta = 1). \quad (17)$$

313 Note that the Gaussian distribution is α -stable with $\alpha = 2$ (in which case the skewness is
 314 irrelevant), making this CLT a true generalization of the classical version.

315 As before, recast the generalized CLT (17) to approximate the sum of random jumps:

$$Y_1 + \dots + Y_n \approx n\mu + \sigma n^{1/\alpha} S_\alpha(0, 1, \alpha, \beta)$$
$$Y_1 + \dots + Y_n \approx t \frac{\mu}{\Delta t} + \frac{\sigma}{\Delta t^{1/\alpha}} t^{1/\alpha} S_\alpha(0, 1, \alpha, \beta)$$
(18)

316
317 and let $v = \frac{\mu}{\Delta t}$ and $\mathcal{D} = \frac{\sigma^\alpha}{\Delta t}$ to find an α -stable density

$$\hat{C}(k, t) = e^{(-vt(ik) + \mathcal{D}t(ik)^\alpha)}$$

318
319 in Fourier space. The α -stable density cannot be written in closed form in real space. A
320 variety of methods exist to estimate the inverse transform numerically [Nolan, 1998].

321 Figure 5(a) illustrates a simple random walk with heavy tailed particle jumps. Figure
322 5(b) shows the same random walk at a longer time scale. Figure 5(c) shows the stable Lévy
323 motion that emerges as the long-time scaling limit of this heavy tailed random walk. The
324 graph of the particle path is a random fractal with dimension $2 - 1/\alpha$. The large jumps
325 seen in the random walk persist in the scaling limit. Figure 6 illustrates the probability
326 density $C(x, t)$ of particle locations for the stable Lévy motion limit process. This particle
327 motion process exhibits a super-diffusive spreading rate, skewness, and power law right
328 tail (early arrivals downstream).

329 The right-hand side of (18) is called α -stable Lévy motion with drift. This limit pro-
330 cess $vt + Z(t)$ represents the location of a randomly selected particle at time $t > 0$,
331 assuming that particle location $x = 0$ at the initial time $t = 0$. The diffusion term
332 $Z(t) = t^{1/\alpha} S_\alpha(0, 1, \alpha, \beta)$ exhibits non-Fickian scaling, a characteristic often seen in lab-
333 oratory and field studies [Benson *et al.*, 2000, 2001]. Since $\alpha < 2$ the scaling factor $t^{1/\alpha}$
334 grows faster (the plume spreads faster) than the classical ADE case $\alpha = 2$, so this model is
335 often called super-diffusive. Aside from its super-Fickian scaling, Lévy motion has other
336 features that distinguish it from its close cousin, Brownian motion. Lévy motion proba-

337 bility densities are positively skewed, with a long leading tail [*Samorodnitsky and Taqqu,*
 338 1994]. In fact, the probability mass a distance r units or more from the plume center of
 339 mass falls off like $x^{-\alpha}$ so that particles are much more likely to race ahead of the mean.

4.2. Eulerian approach to fractional-in-space ADEs

340 The Eulerian approach accounts for bulk mass movements into and out of a finite size
 341 control volume of edge size $\Delta x = h$ during a short time step Δt , as in Figure 7. In a fractal
 342 porous medium (and perhaps, in a fractal river network), the velocity of different particles
 343 in the control volume can vary widely, so that a particle can enter the control volume from
 344 long distances upstream via high velocity paths. The fractal medium imposes a power-
 345 law velocity distribution, leading to a fractional Fick's Law $F = -\mathcal{D}\partial^{\alpha-1}C/\partial x^{\alpha-1}$ for
 346 dispersive flux [*Schumer et al., 2001*], since dispersion comes from variations in velocity.
 347 The Grunwald weights in Figure 1 code the velocity distribution. A fractional dispersive
 348 flux in the solute mass conservation equation (12) leads to a fractional-in-space ADE

$$349 \quad \frac{\partial C(x, t)}{\partial t} = -v \frac{\partial C(x, t)}{\partial x} + \mathcal{D} \frac{\partial^\alpha C(x, t)}{\partial x^\alpha}. \quad (19)$$

Use Fourier transforms to solve the space-fADE (19):

$$\begin{aligned} \frac{\partial \hat{C}(k, t)}{\partial t} &= -v(ik)\hat{C}(k, t) + \mathcal{D}(ik)^\alpha \hat{C}(k, t) \\ \hat{C}(k, t) &= \exp[-vt(ik) + \mathcal{D}t(ik)^\alpha] \end{aligned}$$

350 which is the Fourier transform of an α -stable density with shift $\mu = vt$, spread $\sigma^\alpha = \mathcal{D}t$,
 351 skewness $\beta = 1$, and tail parameter $1 < \alpha \leq 2$. More extreme deviations from the mean
 352 velocity are represented by heavier tailed jump distributions and, in turn, are governed by
 353 fractional ADEs with smaller fractional derivatives on the flux term [*Clarke et al., 2000*].

354 An alternative Eulerian derivation of the space-fADE uses a fractional conservation of
 355 mass with a traditional Fickian flux [*Meerschaert et al., 2006*]. *Ganti et al.* [2009] develop a

356 probabilistic Exner equation for sediment transport, which is applicable when particle step
 357 lengths follow a heavy tailed (power law) pdf. This asymptotic governing equation for the
 358 movement of entrained particles is valid at scales long enough to encompass many particle
 359 jumps. Using an active layer approach, neglecting porosity, and assuming equilibrium
 360 (steady, uniform) bedload transport of grains of uniform size over a bed, the probabilistic
 361 Exner equation in the presence of a heavy tailed step length is $\frac{L_a}{E} \frac{\partial f_a}{\partial t} = -v \frac{\partial f_a}{\partial x} + D \frac{\partial^\alpha f_a}{\partial x^\alpha}$,
 362 where f_a is the fraction of tracer particles in the active layer, v, D are as in the space-
 363 FADE (19), L_a is the thickness of the active layer, and E is the entrainment rate. Dividing
 364 both sides by L_a/E yields an equation mathematically identical to the space-FADE (19),
 365 so that the same solution methods apply.

4.3. Characteristics of space fADE solutions

366 Characteristics of the Green's function solutions to the advection-dispersion equation
 367 with a fractional-order term in space (Fig. 4) are:

- 368 1. Spatial snapshots
 - 369 (i) α -stable concentration profiles are skewed with long right tail
 - 370 (ii) Plume leading edges decays like a power law $x^{-\alpha-1}$
 - 371 (iii) Snapshot width spreads like $t^{1/\alpha}$
 - 372 (iv) Total mass remains constant over time
- 373 2. Flux at position x
 - 374 (i) Asymmetric breakthrough curves
 - 375 (ii) Long leading edge
 - 376 (iii) Breakthrough curve width grows like $x^{1/\alpha}$.

(iv) Area under breakthrough curve remains constant.

5. Fractional-in-time ADEs

378 Tracer particles at the Earth surface spend more time at rest than in motion [*Sadler,*
379 1981; *Leopold et al.*, 1964; *Tipper*, 1983]. For example, frequency distributions of bedload
380 path length are positively skewed, indicating that many particles do not move from the
381 point of tracer input over the measurement period [*Hassan and Church*, 1992; *Pryce and*
382 *Ashmore*, 2003]. Small deviations in waiting times will not affect long term dispersion
383 rates, but heavy-tailed waiting times will. This affects overall bedload rates [*Singh et al.*,
384 2009] and the resulting transport characteristics can be accommodated by time-fractional
385 ADE, which will be developed from both the Lagrangian and Eulerian view. Evidence for
386 heavy-tailed waiting times in transport is captured in the depositional record [*Schumer*
387 *and Jerolmack*, 2009]. A promising avenue for future research is to examine waiting times
388 between entrainment events, to determine whether a time-fractional Exner equation may
389 be useful to incorporate particles outside the active layer, including deeply buried particles,
390 those incorporated into the hyporheic zone, and particles outside the normal flowpath of
391 a river (sandbars, floodplain - e.g. see discussion in *Ganti et al.* [2009]).

5.1. Lagrangian approach to fractional-in-time ADEs

392 A continuous time random walk (CTRW) imposes a random waiting time J_n before the
393 particle jump Y_n occurs. The particle location at time t is

394

$$X(t) = Y_1 + \dots + Y_n$$

395 where $n = N(t)$ is the number of jumps by time t . Suppose the particle jumps have mean
 396 zero so that the centered (generalized) CLT applies:

$$397 \quad Y_1 + \cdots + Y_n \approx n^{1/\alpha} Z$$

398 where Z is stable (normal if $\alpha = 2$). The sum $J_1 + \cdots + J_n$ gives the time of the n th
 399 particle jump. If the waiting times have a finite mean ν then the law of large numbers (8)
 400 shows that the n th jumps happens at time $t = T_n \approx n\nu$ and then $X(t) \approx Y_1 + \cdots + Y_{t/\nu}$
 401 leads to the classical ADE. On the other hand, if the waiting times J_n are heavy-tailed
 402 with power-law index $0 < \gamma < 1$ and scale $\sigma = 1$ then the generalized CLT yields

$$403 \quad \frac{J_1 + \cdots + J_n - n\nu}{n^{1/\gamma}} \rightarrow W, \quad (20)$$

404 where W is distributed like $S_\gamma(\mu = 0, \sigma = 1, \gamma, \beta = 1)$. Since $\gamma < 1$, we find $n\nu/n^{1/\gamma} \rightarrow 0$,
 405 and so the centering term in (20) can be neglected. Then the n th jump occurs at time

$$406 \quad t = J_1 + \cdots + J_n \approx n^{1/\gamma} W \quad (21)$$

407 for large n . Solving for n shows that the particle location $X(t) = Y_1 + \cdots + Y_n \approx n^{1/\alpha} Z$
 408 where $n \approx (t/W)^\gamma$ for large n . Putting this all together, we see that

$$409 \quad X(t) \approx (t/W)^{\gamma/\alpha} Z$$

410 and this approximation is exact in the scaling limit, where the number of jumps tends to
 411 infinity [Meerschaert and Scheffler, 2004]. If $g(t)$ is the pdf of W , a change of variables
 412 [Meerschaert and Scheffler, 2004] shows that $u = (t/W)^\gamma$ has pdf

$$413 \quad q(u, t) = \frac{t}{\gamma} u^{-1-1/\gamma} g(tu^{-1/\gamma})$$

414 for $u > 0$. If $f(x, u)$ is the pdf of $u^{1/\alpha} Z$ then taking a weighted average with respect to
 415 u [Meerschaert and Scheffler, 2004] shows that the limit particle location x at time t has

$$417 \quad C(x, t) = \int_0^\infty f(x, u)q(u, t) du \quad (22)$$

418 a scale mixture of stable densities. Since

$$419 \quad \begin{aligned} \hat{f}(k, u) &= e^{\mathcal{D}u(ik)^\alpha} \\ \tilde{q}(u, t) &= s^{\gamma-1}e^{-us^\gamma} \end{aligned} \quad (23)$$

420 (for the Laplace transform formula, see [Meerschaert and Scheffler, 2002b]) a simple
421 integration shows that the Fourier-Laplace transform of $C(x, t)$ is

$$422 \quad \bar{C}(k, s) = \frac{s^{\gamma-1}}{s^\gamma - \mathcal{D}(ik)^\alpha}$$

423 which will lead to the space-time fractional ADE. Rearrange to get $s^\gamma \bar{C}(k, s) - s^{\gamma-1} =$
424 $\mathcal{D}(ik)^\alpha \bar{C}(k, s)$ and invert the Laplace and Fourier transforms using (7) to get

$$425 \quad \frac{\partial^\gamma C(x, t)}{\partial t^\gamma} = \mathcal{D} \frac{\partial^\alpha C(x, t)}{\partial x^\alpha}$$

426 using the Caputo derivative in time, where the point source initial condition implies
427 $\hat{C}(k, t = 0) = 1$. Adding an advective drift yields the space-time fractional ADE

$$428 \quad \frac{\partial^\gamma C(x, t)}{\partial t^\gamma} = -v \frac{\partial C(x, t)}{\partial x} + \mathcal{D} \frac{\partial^\alpha C(x, t)}{\partial x^\alpha} \quad (24)$$

429 which governs the CTRW particle density in the long-time limit. It is important to note
430 that the parameter α codes the large particle jumps (early arrivals) and γ controls the
431 long waiting times (residence times). A more detailed analysis using the CLT leads to
432 higher order temporal derivatives [Baeumer et al., 2005; Baeumer and Meerschaert, 2007].

433 The limit process $X(t) = Z(T(t))$ is a subordinated Lévy (or Brownian) motion. The
434 outer process is the random walk limit discussed previously. The inner process $T(t) =$
435 $(t/W)^\gamma$ adjusts for the time a randomly selected particle spends in motion (e.g., see recent
436 work by Ganti et al. [2009] who propose a subordinated Brownian motion model for

437 sediment transport). We call $u = T(t)$ the operational time, since it counts the number of
 438 particle jumps by time t . Since the operational time process incorporates memory effects,
 439 it is non-Markovian, and it is simpler to understand its inverse process $t = W(u)$ that
 440 maps operational time back to clock time t . The process $W(u) = u^{1/\gamma}W$ comes from
 441 (21) and it is another Lévy motion with index $\gamma < 1$. Then the operational time process
 442 $u = T(t)$ is the inverse of this Lévy process. The scaling $W(u) = u^{1/\gamma}W$ is consistent with
 443 the inverse scaling $T(t) = t^\gamma T$ already noted. The scaling $X(t) = Z(T(t)) = Z(t^\gamma T) =$
 444 $t^{\gamma/\alpha} Z(T) = t^{\gamma/\alpha} X$ shows that particles following the space-time fractional ADE spread at
 445 rate $t^{\gamma/\alpha}$ which is slower than the ADE if $\alpha = 2$. This model is often called sub-diffusive.
 446 The random time change T has finite moments of all orders, so in the heavy tailed case
 447 $\alpha < 2$ it does not affect the tails of $X(t)$ which still fall off like $x^{-\alpha}$ [Meerschaert and
 448 Scheffler, 2004]. The mixture integral (22) is a weighted average of the PDF $f(x, u)$ of
 449 the random walk limit $Z(u)$ according to the PDF $q(u, t)$ of the inverse Lévy process $T(t)$.

450 Figure 8(a) illustrates a CTRW with heavy tailed waiting times. Figure 8(b) shows the
 451 same CTRW at a longer time scale. Figure 8(c) shows the continuous particle path of the
 452 subordinated Brownian motion that emerges as the long-time scaling limit of this CTRW.
 453 The long resting times (particle retention) seen in the CTRW persist in the scaling limit.

5.2. Eulerian approach to fractional-in-time ADEs

454 The Eulerian approach accounts for bulk mass movements into and out of a control
 455 volume of edge size $\Delta x = h$ during a short time step Δt , as in Figure 7. The time-
 456 fADE includes memory effects, allowing particle residence times for long periods. This
 457 means that particles can enter the control volume at the current time step from locations
 458 *upstream in time* as depicted in Figure 10. A power-law memory function [Haggerty and

459 *Gorelick, 1995; Haggerty et al., 2000, 2002*] implies that the time-flux can be coded using
 460 a discrete convolution in time $\sum C(x, t - jh)w_j$ using the power-law Grunwald weights
 461 from Figure 1. This leads to a time-fractional analogue $n\partial^\gamma C(x, t)/\partial t^\gamma = -\partial F(x, t)/\partial x$
 462 to the conservation of solute mass equation (12) that combines with the usual advective
 463 and dispersive flux equation (13) to produce the time-fADE

$$464 \quad \frac{\partial^\gamma C(x, t)}{\partial t^\gamma} = -v \frac{\partial C(x, t)}{\partial x} + \mathcal{D} \frac{\partial^2 C(x, t)}{\partial x^2}. \quad (25)$$

465 If power-law residence time (memory function) is combined with power-law velocity dis-
 466 tribution, we recover the same space-time fADE (24) derived from the Lagrangian model.
 467 The time-fractional parameter γ codes retention, since it implies that the memory function
 468 $t^{-\gamma}$ is a power law, and so it can be estimated from the late-time tail of the breakthrough
 469 curve [*Schumer et al., 2003*].

470 The solution $C(x, t)$ to the time-fADE (25) is the probability density of the subordinated
 471 process $X(t) = Z(T(t))$ that models the location of a randomly selected particle. The
 472 solution formula (22) mixes the density of $Z(u)$ according to the operational time process
 473 $u = T(t)$. The outer process $Z(u)$ is a Brownian motion connected with the right-hand
 474 side of (25), and the inner process compensates for the memory effects of the fractional
 475 time derivative on the left-hand side of (25).

5.3. Characteristics of time (and space) fADE solutions

476 Characteristics of the Green's function solutions to the advection-dispersion equation
 477 with a fractional-order term in time and possibly space are:

- 478 1. Spatial snapshots

479 (i) Subordinated α -stable concentration profiles are skewed with long right tail if

480 $\alpha < 2$

481 (ii) Plume leading edges decays like a power law $x^{-\alpha-1}$ if $\alpha < 2$

482 (iii) Snapshot width spreads like $t^{\gamma/\alpha}$

483 (iv) Total mass remains constant over time

484 2. Flux at position x

485 (i) Breakthrough curve tail decays as $t^{-\gamma-1}$

486 (ii) Breakthrough curve width grows like $x^{\gamma/\alpha}$

487 (iii) If $\alpha < 2$, immediate spike in flux then strong leading edge.

488 (iv) Area under breakthrough curve is constant with time

5.4. Fractional ADEs for mobile and immobile zones

489 The fractional-in-time ADE describes the evolution of a tracer plume, but does not
490 distinguish between particles moving at the Earth surface (with mobile concentration
491 denoted C_m) and particles that have been immobilized (C_{im}), where $C = n_m C_m + n_{im} C_{im}$
492 (e.g. *Coats and Smith* [1964]), mobile porosity $n_m = 1$ at the surface and immobile
493 porosity n_{im} may be less than 1 if availability of pore space is a control on immobilization
494 of sediment or solute. This is significant because typical sampling methods for surface
495 water and groundwater solute concentration permit only observation of mobile solute
496 concentration. Mobile solute equations can predict absolute solute concentration rather
497 than relative or normalized concentration C/C_0 because they account for mass loss to
498 immobile zones with time [*Schumer et al.*, 2003].

499 Traditional mobile-immobile equations assume that particles move between the mobile
500 and immobile phases at an instantaneous rate proportional to the difference in concen-
501 tration. If particles begin in an immobile phase, this implies that immobile concentration
502 decays exponentially in time, as reflected in the late-time breakthrough curve. A multiple-
503 rate mass transfer model (MRMT) uses a memory function to govern release from the
504 immobile phase [Haggerty and Gorelick, 1995], and has been used to fit late time solute
505 breakthrough curves in groundwater aquifers [Haggerty et al., 2000]. Following [Schumer
506 et al., 2003] we write the MRMT equations for transport:

$$\begin{aligned}
\frac{\partial C_m}{\partial t} + \beta \frac{\partial C_m}{\partial t} \star g(t) &= LC_m - C_m(x, t = 0)\beta g(t) \\
\frac{\partial C_{im}}{\partial t} + \beta \frac{\partial C_{im}}{\partial t} \star g(t) &= LC_{im} + C_m(x, t = 0)g(t)
\end{aligned}
\tag{26}$$

508 where the capacity coefficient $\beta = n_{im}/n_m$, “ \star ” denotes convolution, $g(t)$ is the memory
509 function, and we write $L = -v\partial/\partial x + D\partial^2/\partial x^2$ for brevity. Equations (26) assume that
510 all solute begins in the mobile phase. If power law memory is of form $g(t) = t^{-\gamma}/\Gamma(1-\gamma)$,
511 the memory function convolution becomes the Caputo fractional derivative in time (6),
512 and (26) becomes the fractal mobile-immobile equations

$$\begin{aligned}
\frac{\partial C_m}{\partial t} + \beta \frac{\partial^\gamma C_m}{\partial t^\gamma} &= LC_m - C_{m,0}(x) \frac{\beta t^{-\gamma}}{\Gamma(1-\gamma)} \\
\frac{\partial C_{im}}{\partial t} + \beta \frac{\partial^\gamma C_{im}}{\partial t^\gamma} &= LC_{im} + C_{m,0}(x) \frac{t^{-\gamma}}{\Gamma(1-\gamma)}
\end{aligned}
\tag{27}$$

514 with $C_{m,0}(x) = C_m(x, t = 0)$ as in [Schumer et al., 2003]. Figure 9 shows the characteristic
515 behavior of fractal mobile-immobile transport. The late-time behavior of the breakthrough
516 curve is governed by the order of the time-fractional derivative. The key characteristics
517 of the mobile zone FADE that differ from those of the fractional-in-time ADE are:

- 518 1. Total mass in the mobile zone decays with time as $\frac{t^{\gamma-1}}{\Gamma(\gamma)}$

519 2. If $\alpha < 2$, the breakthrough curve has a long leading edge but no immediate spike in
520 flux.

6. Scaling properties of fractional ADEs

521 The limiting stochastic process governed by any (traditional or fractional) ADE is self-
522 similar and has useful scaling properties. For example, the traditional ADE governs
523 Brownian motion with drift, so that relative concentration $C(x, t)$ in (11) gives the prob-
524 ability density for this stochastic process. There are actually two scales in this equation.
525 The plume center of mass moves linearly, proportional to t , and the plume spreads more
526 slowly, proportional to $t^{1/2}$ as t increases. To focus on the spread, adopt a moving coordi-
527 nate system with origin at the plume center of mass. This converts to $v = 0$ in the ADE,
528 so that it reduces to the diffusion/dispersion equation

$$529 \quad \frac{\partial C(x, t)}{\partial t} = \mathcal{D} \frac{\partial^2 C(x, t)}{\partial x^2} \quad (28)$$

530 whose point source solution is

$$531 \quad C(x, t) = \frac{1}{\sqrt{2\pi \cdot 2\mathcal{D}t}} e^{-\frac{x^2}{2 \cdot 2\mathcal{D}t}} \quad (29)$$

532 a mean zero normal density with variance $2\mathcal{D}t$. A snapshot graph of this density curve
533 for any fixed t is bell-shaped, centered at the origin, and as t increases, the snapshots
534 are all the same shape. This scaling property is expressed mathematically as $C(x, t) =$
535 $t^{-1/2}C(xt^{-1/2}, 1)$ which clearly shows that the concentration snapshot spreads away from
536 its center of mass like $t^{1/2}$ and the plume peak concentration decreases at the same rate.
537 This scaling is also evident in the Fourier transform $\hat{C}(k, t) = \exp[-\mathcal{D}tk^2]$ since evidently
538 $\hat{C}(k, t) = \hat{C}(t^{1/2}k, 1)$. For the space-fADE, the same moving coordinate system leads
539 to $C(x, t) = t^{-1/\alpha}C(xt^{-1/\alpha}, 1)$ and again with $\hat{C}(k, t) = \exp[\mathcal{D}t(ik)^\alpha]$ we have $\hat{C}(k, t) =$

540 $\hat{C}(t^{1/\alpha}k, 1)$. Thus the space-fADE snapshot, a stable density with index α , spreads like
 541 $t^{1/\alpha}$ while its peak falls at the same rate. Solutions to the space-time fADE (24) with
 542 $v = 0$ can be expressed as $\hat{C}(k, t) = E_\gamma(t^\gamma \mathcal{D}(ik)^\alpha)$ [Mainardi and Gorenflo, 2000] where
 543 the Mittag-Leffler function

$$544 \quad E_\gamma(z) = \sum_{k=0}^{\infty} \frac{z^k}{\Gamma(1 + \gamma k)}$$

545 is an extension of the exponential (the special case $\gamma = 1$) used in the theory of time-
 546 fractional equations. It is easy to see that $\hat{C}(k, t) = t^{\gamma/\alpha} \hat{C}(k, 1)$ and so the space-time
 547 fADE is also scale-invariant after mean centering: The plume snapshot spreads like $t^{\gamma/\alpha}$
 548 and the plume peak falls at the same rate [Meerschaert et al., 2002].

549 If a transport model reveals scale dependence of parameters, it is likely that the model
 550 is scale dependent, not the transport process itself. One option is to use a model with
 551 time-dependent parameters, but this is difficult to apply in practice. Using a model
 552 that includes the correct scaling is useful for prediction because its parameters will be
 553 constant in time. In the fractional-in-space and time case, the scaling rate $t^{\gamma/\alpha}$ can be
 554 obtained with non-unique $0 < \gamma \leq 1$ and $1 < \alpha \leq 2$ (for example, a scaling rate of
 555 $t^{0.56}$ can be obtained with $\alpha = 1.8$ and $\gamma = 1$ or $\alpha = 1.5$ and $\gamma = 0.83$). The tail
 556 properties of plume snapshots or breakthrough curves will be necessary to obtain the order
 557 of the space and time fractional derivatives. An analysis of plume moments may also be
 558 necessary for choosing the appropriate transport model [Zhang et al., 2008]. The scaling
 559 rate for plumes following a mobile fractional ADE is [Schumer et al., 2003] $C_m(x, t) =$
 560 $t^{\gamma-1} t^{-\frac{\gamma}{\alpha}} C_m(t^{-\frac{\gamma}{\alpha}} x, 1)$. In summary, fADE plumes spread out from the center of mass
 561 according to precise scaling rates, that are determined by the order of the space or time
 562 derivative. A smaller index α on the space derivative implies faster (super-dispersive)

563 spreading, while a smaller γ index on the time derivative yields a slower (sub-dispersive)
 564 spread. In practice, the super-dispersive effect comes from high velocity contrasts, while
 565 the sub-diffusive behavior reflects long residence times.

7. CTRW derivation of the space-time fADE

566 The Lagrangian derivation of the space-time fADE is closely connected to the underlying
 567 CTRW model for particle transport [Berkowitz *et al.*, 2002, 2006]. Each random particle
 568 jump Y_n follows a random waiting time J_n . Suppose that Y_n has mean v and $P(Y_n - v >$
 569 $x) \approx x^{-\alpha}$ and $P(J_n > t) \approx t^{-\gamma}$ for large x and t . Then the jump pdf $p(x)$ of Y_n has
 570 Fourier transform $\hat{p}(k) = 1 - ikv + \mathcal{D}(ik)^\alpha + \dots$ and the waiting time pdf $\psi(t)$ of J_n
 571 has Laplace transform $\tilde{\psi}(s) = 1 - s^\gamma + \dots$ where we emphasize the dominant terms for
 572 small k and s . The master equation (Montroll and Weiss [1965]; Scher and Lax [1973],
 573 also used in Furbish *et al.* [2009a, b] to describe probability of soil particle flux) gives the
 574 Fourier-Laplace transform of the CTRW particle density :

$$575 \quad \bar{C}(k, s) = \frac{1 - \tilde{\psi}(s)}{s} \frac{1}{1 - \hat{p}(k)\tilde{\psi}(s)} \quad (30)$$

576 After substituting power-law space and time jump pdfs into the master equation, we find

$$577 \quad \bar{C}(k, s) \approx \frac{s^{\gamma-1}}{s^\gamma + ikv - \mathcal{D}(ik)^\alpha} \quad (31)$$

578 which rearranges to

$$579 \quad s^\gamma \bar{C}(k, s) - s^{\gamma-1} = -ikv \bar{C}(k, s) + \mathcal{D}(ik)^\alpha \bar{C}(k, s).$$

580 Invert the Fourier and Laplace transforms to recover the space-time fADE (24). For
 581 light-tailed particle jumps, the Fourier transform $\hat{p}(k) = 1 - ikv + \mathcal{D}(ik)^2 + \dots$ and the
 582 second derivative in space reappears. For light-tailed waiting times, the Laplace transform

583 $\tilde{\psi}(s) = 1 - s + \dots$ leading to the first derivative in time. The asymptotic approximation
584 is identical to our earlier discussion, and it is only in the limit that the neglected terms
585 vanish to produce the fADE (or the ADE). If the jump length and residence time densities
586 are known exactly, it is possible to model transport with a discrete CTRW without taking
587 the long time or scaling limit simply by using those densities in Equation (30). In this
588 case, a pre-ergodic solution is reached that does not necessarily have scale invariance.

8. Relationship with other stochastic models

589 Fractional ADEs are related to other general stochastic process models of random par-
590 ticle motion. Here we give a brief discussion to provide context. The CTRW master
591 equation (30) inverts to an integral equation for particle density $C(x, t)$ which is also
592 known as the (generalized) master equation [Klafter and Sibley, 1980]. The convolution
593 integral in this master equation can approximate fractional derivatives in space and/or
594 time. The solution to this master equation gives the pdf of the CTRW particle den-
595 sity. The underlying particle motion process consists of space-time jumps as shown in
596 Figures 2(a), 5(a), or 8(a). Fractional advection-dispersion equations arise in the scaling
597 limit. A different approach based on statistical mechanics leads to a continuously evolving
598 stochastic model for particle motion, where particle flux is represented as a convolution
599 integral [Cushman, 1997]. The space-time convolution can capture memory effects (time
600 convolution) and non-local super-diffusive particle jumps (space convolution). The space-
601 time fractional diffusion equation is a special case of this stochastic model, in which the
602 convolution kernel is a power law [Cushman and Ginn, 2000]. A more complex but corre-
603 spondingly general theory is reviewed in Neuman and Tartakovsky [2009]. That paper also
604 compares and contrasts the various theories used in stochastic hydrology in more detail.

605 The added generality allows a velocity field that varies in space and time [*Neuman, 1990*].
606 The variable coefficient fractional ADE represents the special case of a power-law memory
607 kernel in space and time. In any given situation, the practitioner will make an intelligent
608 model selection that takes into account a trade-off between simplicity and generality. For
609 example, it is possible to generate stochastic processes with non-stationary increments
610 that have heavy tails and satisfy classical ADEs with time dependent dispersion tensors
611 [*Berkowitz et al., 2002*]. In our view, fractional advection dispersion equations represent
612 the simplest model that incorporates the anomalous spreading and skewness often seen
613 in transport at the Earth surface. They complement CTRW and other more detailed
614 stochastic models with a simplified (limit) case appropriate for plume modeling at the
615 large scale.

9. Summary- Use of fractional ADEs in modeling Earth surface transport

616 Characterizing the collective behavior of particle transport on the Earth surface is a key
617 ingredient for describing landscape evolution. Alternatives to local, diffusive transport
618 laws are sought because these classical models do not always capture essential features of
619 transport on hillslopes, valleys, river channels, or river networks. Fractional ADEs that
620 can incorporate non-local effects in space are now used to describe anomalous transport of
621 sediment which can arise from particle size [*Ganti et al., 2009; Hill et al., 2009*] and flow
622 field variation [*Stark et al., 2009; Bradley et al., 2009*] in streams or disturbance events on
623 hillslopes that mobilize colluvium over a wide range of scales [*Foufoula-Georgiou et al.,*
624 *2009*]. Fractional ADEs that incorporate non-local effects in time can reproduce power-
625 law residence times and loss to immobile zones that arise because tracer particles spend
626 more time at rest than in motion at the Earth surface. These macroscopic equations arise

627 from characteristic particle ‘hop’ behaviors (Figure 11). In the Lagrangian picture, when
628 the probability of a long hop falls off like $x^{-\alpha}$ then the α -order fractional derivative in
629 space emerges. If the likelihood of a long residence time falls off like $t^{-\gamma}$ then a γ -fractional
630 derivative in time appears. From an Eulerian viewpoint, fractional derivatives in space
631 allow the possibility of high velocity contrast, and fractional time derivatives model long
632 power-law residence times. Space or time terms in ADEs with fractional derivatives result
633 in solutions with flexible scaling rates. In real applications, the fractional paradigm often
634 allows the practitioner to replace scale-dependent ADE parameters by scale-independent
635 their fADE analogues.

636 **Acknowledgments.** David Furbish contributed to the introduction to make the
637 manuscript more compelling to Earth surface scientists. His comments, as well as those
638 of Efi Foufoula-Georgiou and two anonymous reviewers led to great improvement of this
639 manuscript. The authors would like to thank NCED (National Center for Earth-surface
640 Dynamics – an NSF Science and Technology Center at the University of Minnesota funded
641 under agreement EAR-0120914) and the Water Cycle Dynamics in a Changing Environ-
642 ment hydrologic synthesis project (University of Illinois, funded under agreement EAR-
643 0636043) for co-sponsoring the STRESS (Stochastic Transport and Emerging Scaling on
644 Earth’s Surface) working group meeting (Lake Tahoe, November 2007) that fostered the
645 research presented here. RAS was partially supported by NSF/Nevada EPSCOR grant
646 EPS-0447416 and NSF grant EAR-0817073. MMM was partially supported by NSF grants
647 EAR-0823965 and DMS-0803360.

References

- 648 Arfken, G., and H. Weber (1995), *Mathematical Methods for Physicists*, Academic Press,
649 San Diego.
- 650 Baeumer, B., and M. M. Meerschaert (2007), Fractional diffusion with two time scales,
651 *Physica A-Statistical Mechanics and Its Applications*, 373, 237–251.
- 652 Baeumer, B., D. Benson, and M. Meerschaert (2005), Advection and dispersion in time
653 and space, *Physica A*, 350(2-4), 245–262.
- 654 Benson, D. A., S. W. Wheatcraft, and M. M. Meerschaert (2000), Application of a frac-
655 tional advection-dispersion equation, *Water Resour. Res.*, 36(6), 1403–1412.
- 656 Benson, D., S. Wheatcraft, and M. Meerschaert (2000), The fractional-order governing
657 equation of Lévy motion, *Water Resour. Res.*, 36(6), 1413–1423.
- 658 Benson, D. A. (1998), The fractional advection-dispersion equation: development and
659 application, Ph.d., University of Nevada.
- 660 Benson, D. A., R. Schumer, M. M. Meerschaert, and S. W. Wheatcraft (2001), Fractional
661 dispersion, Lévy motion, and the made tracer tests, *Trans. Por. Media*, 42, 211–240.
- 662 Berkowitz, B., J. Klafter, R. Metzler, and H. Scher (2002), Physical pictures of transport
663 in heterogeneous media: Advection-dispersion, random-walk, and fractional derivative
664 formulations, *Water Resour. Res.*, 38(10), 1191, doi:10.1029/2001WR001030.
- 665 Berkowitz, B., A. Cortis, M. Dentz, and H. Scher (2006), Modeling non-Fickian transport
666 in geological formations as a continuous time random walk, *Rev. Geophys.*, 44, RG2003,
667 doi:10.1029/2005RG000178.
- 668 Bradley, D., G. Tucker, and D. Benson (2009), Anomalous dispersion in a sand-bed river,
669 *Journal of Geophys. Res. - Earth Surface*, this issue.

670 Clarke, D.D., M.M. Meerschaert, and S.W. Wheatcraft (2005), Fractal Travel Time Esti-
671 mates for Dispersive Contaminants, *Ground Water* 43(3), 401–407.

672 Coats, K. H., and B. Smith (1964), Dead-end pore volume and dispersion in porous media,
673 *J. Soc. Pet. Eng.*, 4, 73–84.

674 Culling, W. (1960), Analytical theory of erosion, *J. Geology*, 68, 336–344.

675 Cushman, J. H. (1997) *The physics of fluids in hierarchical porous media: Angstroms to*
676 *miles*. Kluwer Academic, New York.

677 Cushman, J. H., and T. R. Ginn (2000) Fractional Advection-Dispersion Equation: A
678 Classical Mass Balance With Convolution-Fickian Flux. *Water Resour. Res.* 36(12),
679 3763-3766.

680 Cushman, J., and T. Ginn (1993), Nonlocal dispersion in media with continuously evolving
681 scales of heterogeneity, *Trans. Por. Media*, 13, 123–138.

682 Dietrich, W. E., D. Bellugi, A. Heimsath, J. Roering, J. Sklar, and J. Stock (2003),
683 Geomorphic transport laws for predicting landscape form and dynamics, in *Prediction*
684 *in Geomorphology, Geophysical Monograph Series*, vol. 136, edited by P. Wilcock and
685 R. Iverson, AGU, Washington. D.C.

686 Einstein H. (1937), Bed load transport as a probability problem (in German), PhD thesis,
687 Eidgenoess. Tech. Hochsch, Zürich, Switzerland. English translation by W.W. Sayre in
688 *Sedimentation*, edited by H.W. Shen, Appendix C, Fort Collins, Colo., 1972.

689 Feller, W. (1971), *An Introduction to Probability Theory and Its Applications, Wiley Series*
690 *in Probability and Mathematical Statistics*, vol. Vol. II, 2nd ed., Wiley, New York.

691 Foufoula-Georgiou, E., V. Ganti, and W. E. Dietrich (2009), A non-local theory for sedi-
692 ment transport on hillslopes, *Journal of Geophys. Res. - Earth Surface*, this issue.

693 Furbish, D., E. Childs, P. Haff, and M. W. Schmeckle (2009a), Rain splash of soil grains
694 as a stochastic advection-dispersion process, with implications for desert plant-soil in-
695 teractions and land-surface evolution, *JGR-ES*, 114.

696 Furbish, D., P. Haff, W. Dietrich, and A. Heimsath (2009b), Statistical description of
697 slope-dependent soil transport and the diffusion-like coefficient, *JGR-ES*, 114.

698 Ganti, V., M. M. Meerschaert, E. Foufoula-Georgiou, E. Viparelli, and G. Parker, Normal
699 and Anomalous Dispersion of Gravel Tracer Particles in Rivers, *J. Geophys. Res. Earth*
700 *Surface*, in review.

701 Ganti, V., A. Singh, P. Passalacqua, and E. Foufoula-Georgiou (2009), Subordinated
702 brownian motion model for sediment transport, *Phys. Rev. E*, 79(1), in press.

703 Gnedenko, B., and A. Kolmogorov (1968), *Limit Distributions for Sums of Independent*
704 *Random Variables*, Translated from the Russian, annotated, and revised by K.L. Chung.
705 With appendices by J.L. Doob and P.L. Hsu. Revised edition, Addison-Wesley, Reading,
706 Mass.

707 Gooseff, M. N., S. M. Wondzell, R. Haggerty, and J. Anderson (2003), Comparing tran-
708 sient storage modeling and residence time distribution (rtd) analysis in geomorphically
709 varied reaches in the lookout creek basin, oregon usa, *Advances in Water Resources*, 26,
710 925–937.

711 Haggerty, R. and S.M. Gorelick (1995), Multiple-rate mass transfer for modeling diffusion
712 and surface reactions in media with pore-scale heterogeneity, *Water Resour. Res.*,
713 31(10), 2383–2400.

714 Haggerty, R., S. A. McKenna, and L. C. Meigs (2000), On the late-time behavior of tracer
715 test breakthrough curves, *Water Resour. Res.*, 36(12), 34673479.

716 Haggerty, R., S. M. Wondzell, and M. A. Johnson (2002), Power-law residence time dis-
717 tribution in the hyporheic zone of a 2nd-order mountain stream, *Geophys. Res. Lett.*,
718 29(13), 1640, doi:10.1029/2002GL014743.

719 Haggerty, R., C. F. Harvey, C. F. von Schwerin, and L. C. Meigs (2004), What controls
720 the apparent timescale of solute mass transfer in aquifers and soils? a comparison of
721 experimental results, *Water Resources Research*, 40(1).

722 Hassan, M.A. and M. Church (1992) The movement of individual grains on the streambed,
723 In: Billi, P., Hey, R.D., Thorne, C.R., Tacconi, P. (Eds.), *Dynamics of Gravel-Bed*
724 *Rivers*. Wiley, Chichester, UK, pp 159–175.

725 Hill, K.M., L. Dell'Angelo, and M.M. Meerschaert, Particle Size Dependence of the Proba-
726 bility Distribution Functions of Travel Distances of Gravel Particles in Bedload Trans-
727 port, *J. Geophys. Res. Earth Surface*, in review.

728 Klafter, J. and R. Silbey (1980) Derivation of continuous-time random walk equation.
729 *Phys. Rev. Lett.* 44(2), 55–58.

730 Leopold, L., M. Wolman, and J. Miller (1964), *Fluvial processes in geomorphology*, W.H.
731 Freeman, San Francisco, CA.

732 Mainardi, F. (1997), Fractional calculus: some basic problems in continuum and statistical
733 mechanics, in *Fractals and Fractional Calculus in Continuum Mechanics*, edited by
734 A. Carpinteri and F. Mainardi, pp. 292–348, Springer, New York.

735 Mainardi, F. and R. Gorenflo, On Mittag-Leffler-type functions in fractional evolution
736 processes, *J. Comput. Appl. Math.* 118 (2000), 283–299.

737 Malmon, D. V., T. Dunne, and S. L. Reneau (2002), Predicting the fate of sediment and
738 pollutants in river floodplains, *Environmental Science & Technology*, 36(9), 2026–2032.

739 Malmon, D. V., T. Dunne, and S. L. Reneau (2003), Stochastic theory of particle trajec-
740 tories through alluvial valley floors, *Journal of Geology*, *111*(5), 525–542.

741 Mandelbrot, B. (1982), *The Fractal Geometry of Nature*, Freeman, San Francisco.

742 Meerschaert, M.M. and H.P. Scheffler (2001) *Limit Distributions for Sums of Independent*
743 *Random Vectors: Heavy Tails in Theory and Practice*. Wiley Interscience, New York.

744 Meerschaert, M.M. and H.P. Scheffler (2002) Semistable Lévy Motion, *Fractional Calculus*
745 *and Applied Analysis* **5**, 27–54.

746 Meerschaert, M.M., D.A. Benson, H.P. Scheffler and B. Baeumer (2002) Stochastic solu-
747 tion of space-time fractional diffusion equations. *Phys. Rev. E* **65**, 1103–1106.

748 Meerschaert, M., and H.-P. Scheffler (2004), Limit theorems for continuous time random
749 walks with infinite mean waiting times, *J. Applied Probability*, *41*, 623–638.

750 Meerschaert, M., D. Benson, H. Scheffler, and P. Becker-Kern (2002), Governing equations
751 and solutions of anomalous random walk limits, *Phys. Rev. E*, *66*(6), 060,102(4), 102–
752 105.

753 Meerschaert, M. and C. Tadjeran (2004) Finite difference approximations for fractional
754 advection-dispersion flow equations. *J. Comput. Appl. Math.* **172**, 65–77.

755 Meerschaert, M., H.P. Scheffler and C. Tadjeran (2006) Finite difference methods for
756 two-dimensional fractional dispersion equation. *J. Comput. Phys.* **211**, 249–261.

757 Meerschaert, M. M., J. Mortensen, and S. W. Wheatcraft (2006), Fractional vector cal-
758 culus for fractional advection-dispersion, *Physica A-Statistical Mechanics and Its Ap-*
759 *plications*, *367*, 181–190.

760 Montroll, E., and G. Weiss (1965), Random walks on lattices. ii, *J. Math Phys.*, *6*(2),
761 167–181.

762 Neuman, S. P., and D. M. Tartakovsky (2009), Perspective on theories of non-fickian
763 transport in heterogeneous media, *Advances in Water Resources*, 32(5), 670–680.

764 Neuman, S. P. (1990) Universal scaling of hydraulic conductivities and dispersivities in
765 geologic media. *Water Resour. Res.* 26, 1749-1758.

766 Nikora, V., J. Heald, D. Goring, and I. McEwan (2001), Diffusion of saltating particles in
767 unidirectional water flow over a rough granular bed, *Journal of Physics A-Mathematical
768 and General*, 34(50), L743–L749.

769 Nikora, V., H. Habersack, T. Huber, and I. McEwan (2002), On bed particle diffusion in
770 gravel bed flows under weak bed load transport, *Water Resources Research*, 38(6).

771 Nolan, J. P. (1998), Multivariate stable distributions: approximation, estimation, simula-
772 tion and identification, in *A Practical Guide to Heavy Tails: Statistical Techniques and
773 Applications*, edited by R. Adler, R. Feldman, and M. Taqqu, Birkhauser, Boston.

774 Parker, G., C. Paola, and S. Leclair (2000), Probabilistic exner sediment continuity equa-
775 tion for mixtures with no active layer, *Journal of Hydraulic Engineering-Asce*, 126(11),
776 818–826.

777 Pryce, R.S. and P.E. Ashmore (2003) The relation between particle path length distribu-
778 tions and channel morphology in gravel-bed streams: a synthesis, *Geomorphology*, 56,
779 167–187.

780 Sadler, P. M. (1981), Sediment accumulation rates and the completeness of stratigraphic
781 sections, *Journal of Geology*, 89(5), 569–584.

782 Samko, S. G., A. A. Kilbas, and O. I. Marichev (1993), *Fractional Integrals and Deriva-
783 tives: Theory and Applications*, Gordon and Breach, London.

784 Samorodnitsky, G., and M. S. Taqqu (1994), *Stable Non-Gaussian Random Processes:*
785 *Stochastic Models with Infinite Variance*, Stochastic Modeling, Chapman Hall, London.

786 Sayre, W. and D. Hubbell (1965), Transport and dispersion of labeled bed material: North
787 Loup River, Nebraska. US Geological Survey Professional Paper 433-C.

788 Scher, H., and M. Lax (1973), Stochastic transport in a disordered solid. i. theory, *Physical*
789 *Review B*, 7(10), 4491–4502.

790 Schumer, R., D. A. Benson, M. M. Meerschaert, and S. W. Wheatcraft (2001), Eulerian
791 derivation for the fractional advection-dispersion equation, *Journal of Contaminant*
792 *Hydrology*, 48, 69–88.

793 Schumer, R., D. A. Benson, M. M. Meerschaert, and B. Baeumer (2003), Fractal mo-
794 bile/immobile solute transport, *Water Resources Research*, 39(10).

795 Schumer, R., and D. Jerolmack (2009), Real and apparent changes in sediment deposition
796 rates through time, *Journal of Geophys. Res. - Earth Surface*, in review.

797 Singh, A., K. Fienberg, D. J. Jerolmack, J. Marr, and E. Foufoula-Georgiou (2009),
798 Experimental evidence for statistical scaling and intermittency in sediment transport
799 rates, *Journal of Geophysical Research-Earth Surface*, 114.

800 Stark, C., E. Foufoula-Georgiou, and V. Ganti (2009), A nonlocal theory of sediment
801 buffering and bedrock channel evolution, *J. Geophys. Res.*, 114(F01029).

802 Tadjeran, C., M.M. Meerschaert, and H.P. Scheffler (2006) A second order accurate nu-
803 merical approximation for the fractional diffusion equation. *J. Comput. Phys.* **213**,
804 205–213.

805 Tipper, J. C. (1983), Rates of sedimentation and stratigraphical completeness, *Nature*,
806 302(5910), 696–698.

- 807 Worman, A., A. I. Packman, L. Marklund, J. W. Harvey, and S. H. Stone (2007), Fractal
808 topography and subsurface water flows from fluvial bedforms to the continental shield,
809 *Geophysical Research Letters*, *34*(7).
- 810 Zhang, Y., D. A. Benson, M. M. Meerschaert, and H. P. Scheffler (2006) On using random
811 walks to solve the space-fractional advection-dispersion equations. *Journal of Statistical*
812 *Physics*, **123**(1), 89–110.
- 813 Zhang, Y., D.A. Benson, and B. Baeumer (2008) Moment analysis for spatiotemporal
814 fractional dispersion. *Water Resources Research*, *44*(4).

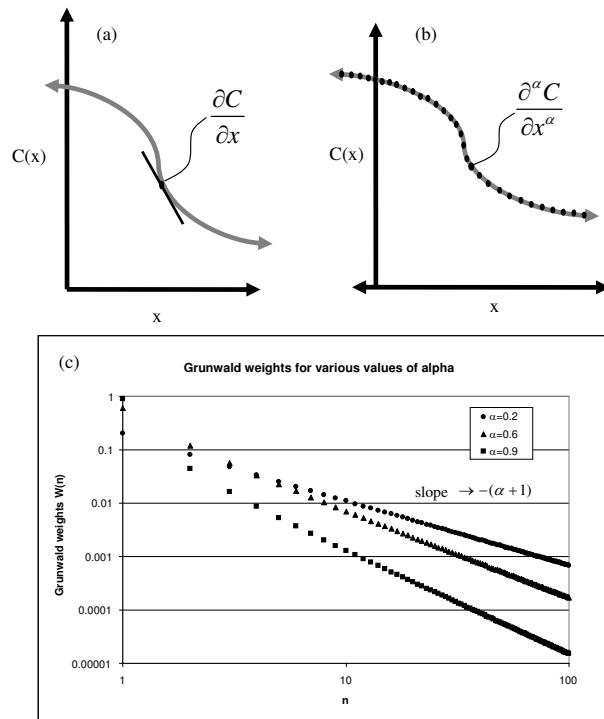
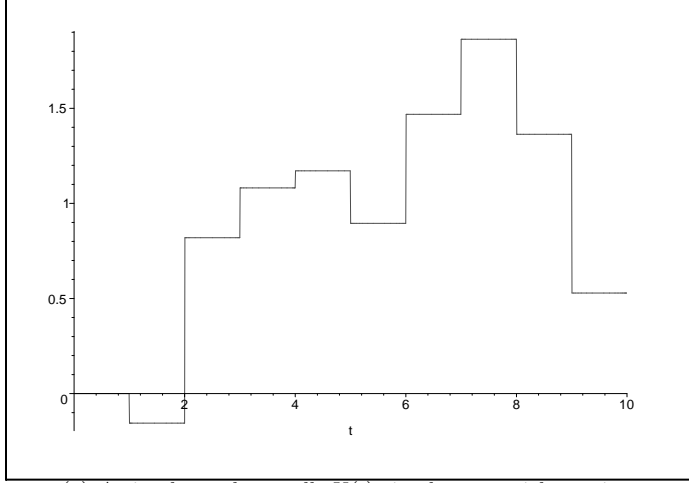
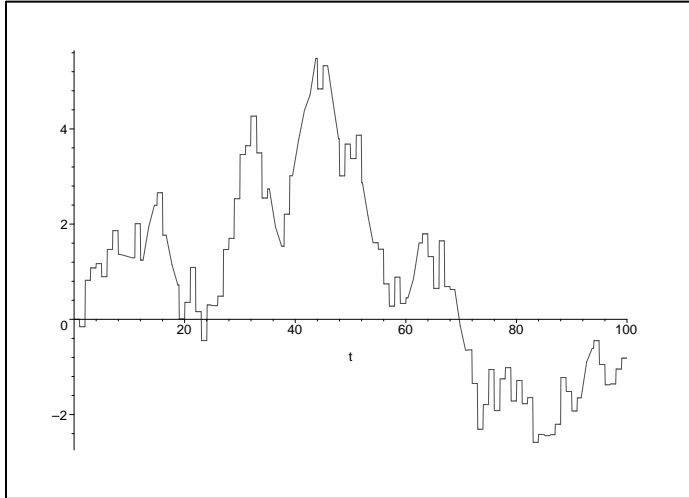


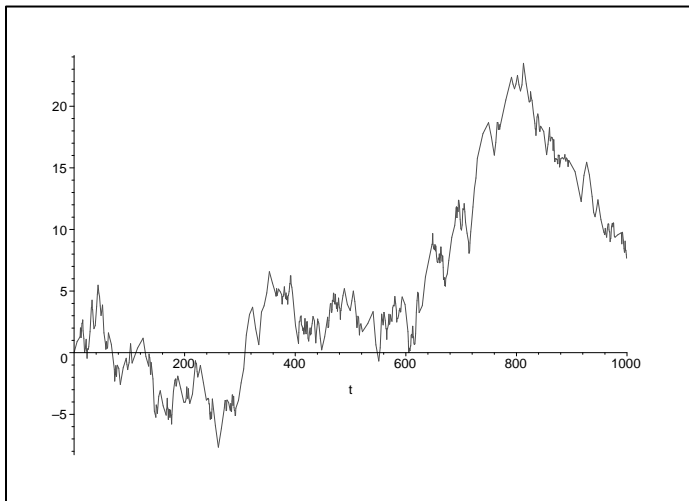
Figure 1. The usual derivative (a) is local but the fractional derivative (b) is non-local. The log-log plot (c) demonstrates the power law decay in Grunwald weights.



(a) A simple random walk $X(t)$ simulates particle motion.



(b) Simple random walk $X(t)$ at a longer time scale.



(c) Brownian motion as the scaling limit of a random walk $X(t)$. Particle graph is a random fractal with dimension $3/2$.

Figure 2. Comparison of random walk traces at increasing time scale and in the scaling limit as a Brownian motion.

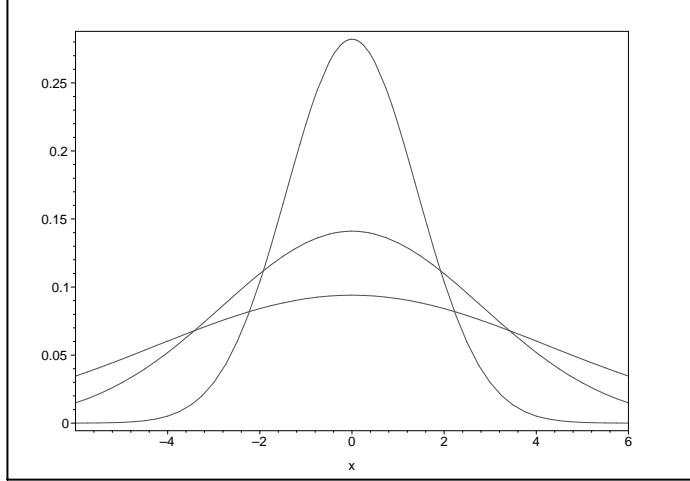


Figure 3. Brownian motion density function $C(x, t)$ describing particle spreading away from plume center of mass at time $t = 1, 4, 9$ in the scaling limit. Note the square root spreading rate and fast tail decay.

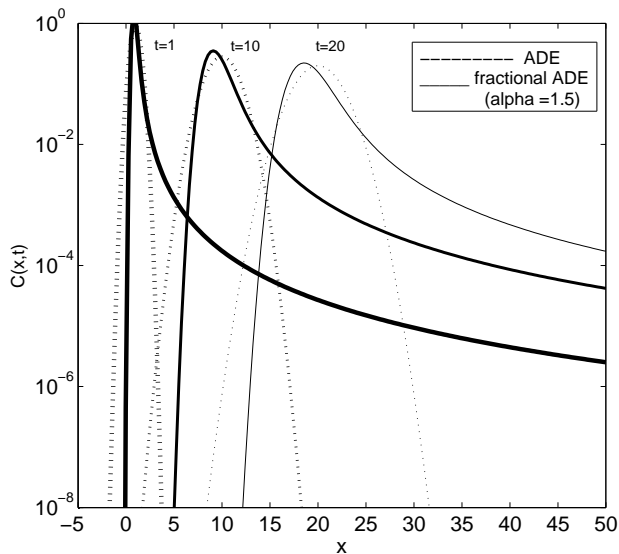
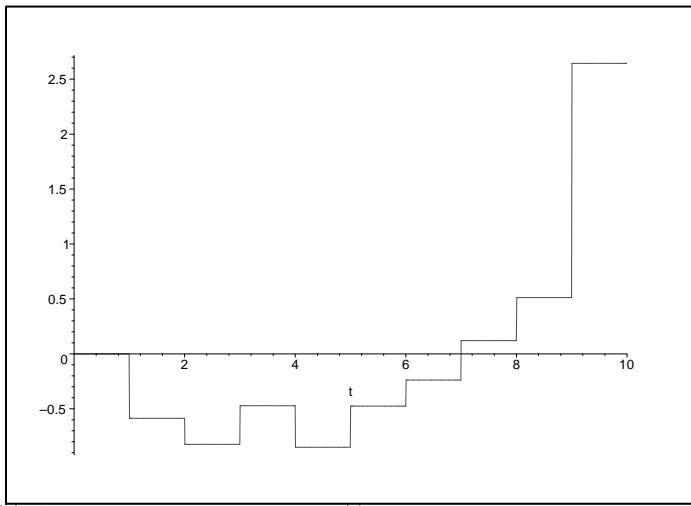
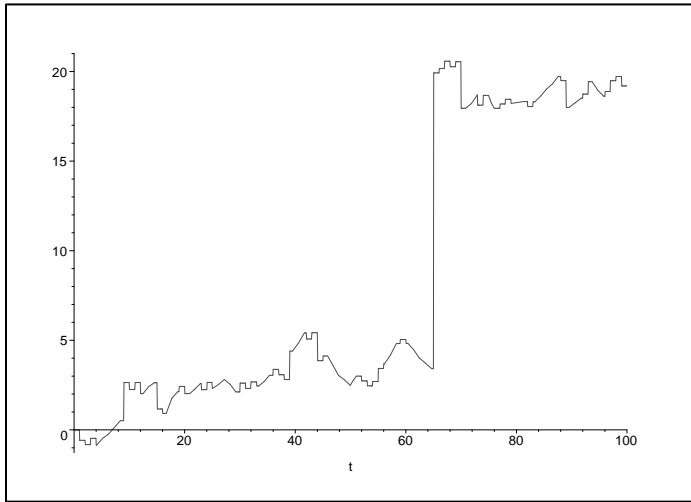


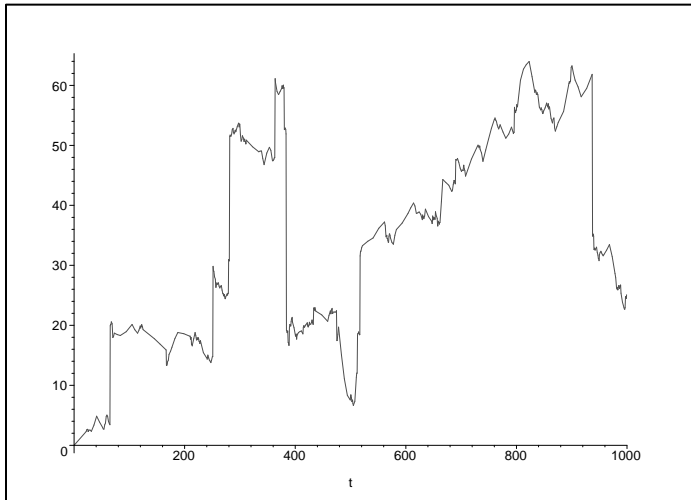
Figure 4. Comparison of the solutions in space to integer-order and fractional ADEs at time $t = 1, t = 10,$ and $t = 20$. For both models, $v = 1$ and $D = 0.1$. The heavy leading edges of the α -stable solutions to the fractional ADE decay as $C(x) \approx x^{-\alpha-1}$.



(a) A heavy tailed random walk $X(t)$ simulates anomalous particle motion.



(b) Heavy tailed random walk $X(t)$ at a longer time scale.



(c) Stable Lévy motion as the scaling limit of a random walk $X(t)$. Particle graph is a random fractal with heavy tailed jumps.

Figure 5. Comparison of heavy tailed random walk traces at increasing time scale and

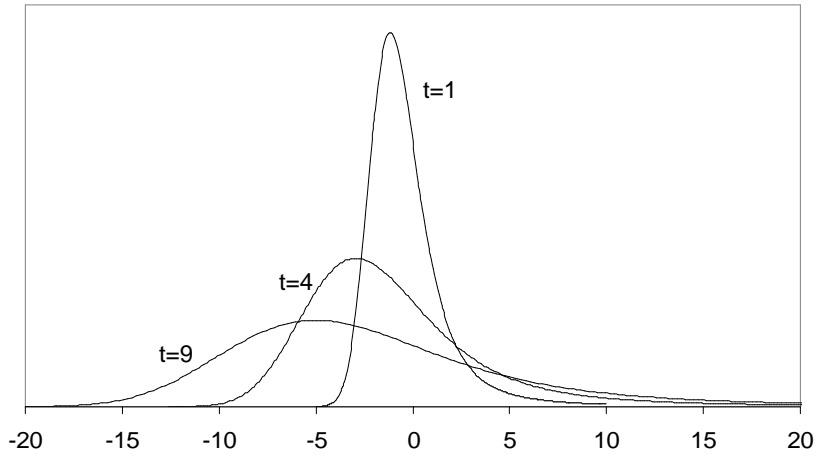


Figure 6. Lévy motion density function $C(x, t)$ describing particle spreading away from plume center of mass at time $t = 1, 4, 9$ in the scaling limit. Note the super-diffusive spreading rate, skewness, and power law tail.

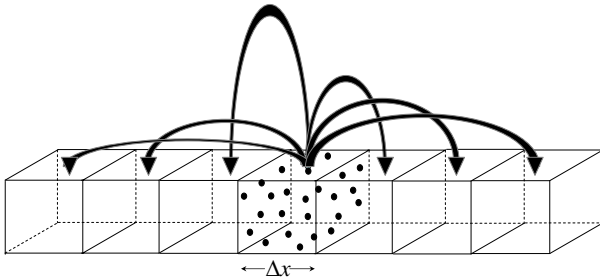
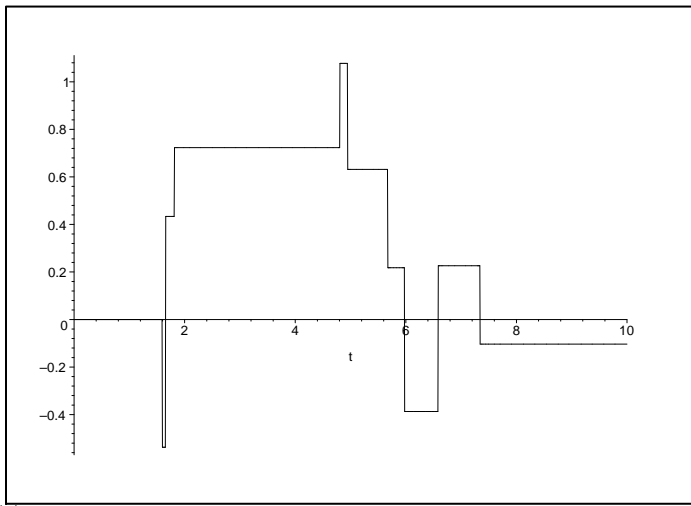
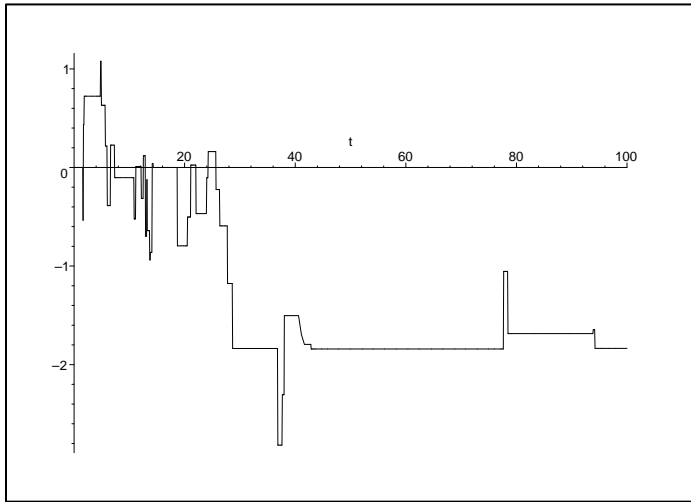


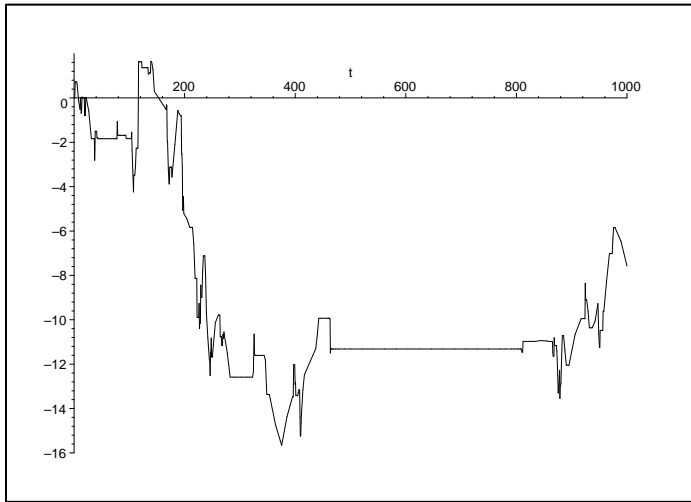
Figure 7. When governed by a fractional-in-space ADE, particle hop length during a small time step Δt may be much larger than the mean size. In finite-difference implementations for fractional ADEs, probability of particle hop length decays as a power law with distance. (After *Schumer et al.* [2001].)



(a) CTRW with heavy tailed waiting times simulates sub-diffusive particle motion.



(b) CTRW at a longer time scale.



(c) Subordinated Brownian motion as the CTRW scaling limit. Long resting times persist in the limit process.

Figure 8. Comparison of heavy tailed waiting time CTRW traces at increasing time

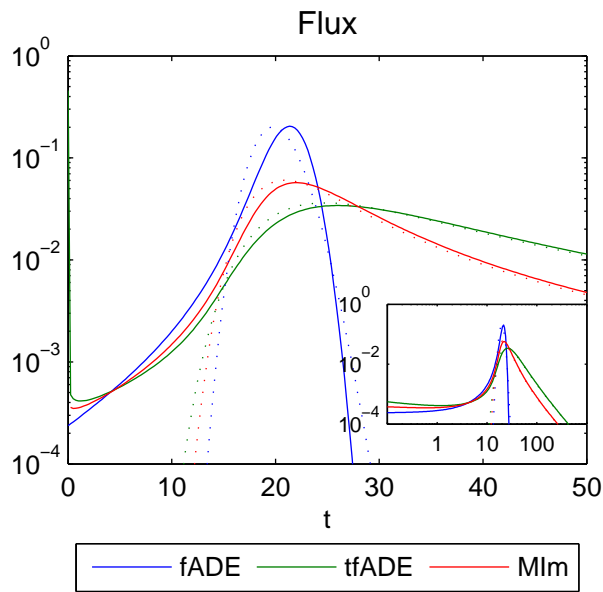


Figure 9. Flux at a distance of $x = 20$ vs. time in semi-log and log-log plots for solutions to equations (19), (23) and (26) with $v = 1$, $D = 0.1$, $\gamma = 0.8$ and $\beta = 1$ where applicable. Dotted lines represent the flux with $\alpha = 2$, solid lines have $\alpha = 1.5$.

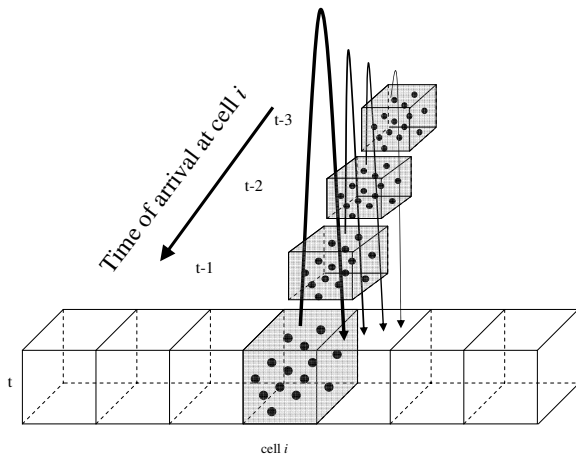


Figure 10. When governed by a fractional-in-time ADE, particles have memory of the time that they arrive at a given point. Their probability of release decays as a power law from arrival time.

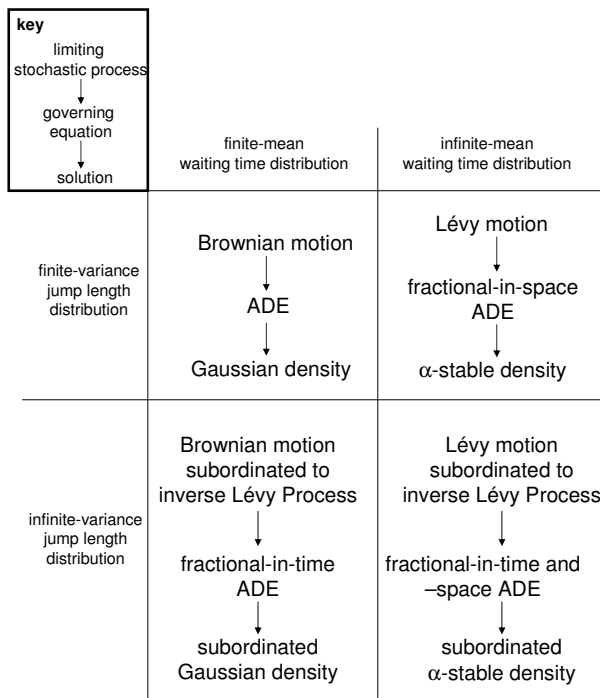


Figure 11. CTRW converge to different limiting stochastic process depending on the tail characteristics of the jump length distribution and waiting time distribution. Particles undergoing the limiting stochastic process are governed by ADEs with either integer-order or non-integer-order derivatives with solutions that are related to probability density functions. A CTRW with finite-mean waiting time distribution converges in the scaling limit to the same stochastic process as the analogous random walk.